Original Paper

Manufacture of short-fibre reinforced glasses by extrusion and examinations regarding their structure and their mechanical properties[1])

Klaus Langhans[2]) and Erwin Roeder
Lehrstuhl für Werkstoffkunde und Mechanische Technologie, Universität Kaiserslautern (FRG)

Technical applications of glasses are mainly limited by their well-known tendency to brittle fracture. One promising possibility to improve the mechanical properties of glasses is the embedding of high-strength reinforcement fibres for increasing the strength and, first of all, the fracture toughness of these materials. Therefore, new fields of application for these glasses can be developed, where their many favourable properties become effective.

In this paper the manufacture – by extrusion – of short-fibre reinforced glasses as well as structural and mechanical examinations of the thus produced specimens are represented. Due to the manufacturing process, extrusion results in a nearly unidirectional orientation of the fibres, parallel to the axis of the rod, with a corresponding high degree of reinforcement. After the explanation of the theoretical fundamentals of short-fibre reinforcement of brittle materials, the properties of the materials used for the experiments and the manufacture of the composites are described in detail. The subsequently illustrated examinations have clearly shown improvements of the mechanical properties of the glasses as well as good accordance with the theoretical considerations.

Herstellung kurzfaserverstärkter Gläser durch das Strangpreßverfahren und Untersuchungen zu ihrer Struktur und ihren mechanischen Eigenschaften

Die technische Anwendung von Gläsern wird in erster Linie durch ihre bekanntermaßen hohe Sprödbruchneigung eingeschränkt. Eine aussichtsreiche Möglichkeit, die mechanischen Eigenschaften von Gläsern zu verbessern, bietet die Einlagerung hochfester Verstärkungsfasern zur Erhöhung der Festigkeit sowie vor allem der Bruchzähigkeit dieser Werkstoffe. Dadurch können diesen Materialien neue Anwendungsgebiete erschlossen werden, in denen ihre zahlreichen vorteilhaften Eigenschaften zur Geltung kommen.

In der vorliegenden Arbeit werden die Herstellung kurzfaserverstärkter Gläser mittels des Strangpreßverfahrens sowie strukturelle und mechanische Untersuchungen der dabei erhaltenen Probestäbe dargestellt. Das Strangpressen führt verfahrensbedingt zu einer nahezu unidirektionalen achsparallelen Ausrichtung der Kurzfasern im Strang mit entsprechend hoher Verstärkungswirkung. Nach der Darstellung der theoretischen Grundlagen der Kurzfaserverstärkung spröder Materialien werden die Eigenschaften der verwendeten Versuchswerkstoffe und die Herstellung der Verbunde eingehend beschrieben. In den anschließend erläuterten Untersuchungen der Verbundproben konnten sowohl deutliche Eigenschaftsverbesserungen der Gläser als auch gute Übereinstimmungen mit den theoretischen Betrachtungen festgestellt werden.

1. Introduction

Although glasses show some excellent properties, their practical use today chiefly is limited to optical applications, articles of daily use and some branches of the chemical industry and laboratory techniques. The main reason for this situation is their strong tendency to brittle fracture. The other properties, however, make efforts to find new applications for these materials worthwhile. Here, only the very high degree of chemical resistance, the excellent hardness and wear resistance, the low density, and the limited thermal stability of glasses should be mentioned. As, however, the brittleness of glass is a result of its structure and can be influenced only in a very restricted way, intensive efforts have been made in the last few years to improve the fracture behaviour by embedding fibres with both high strength and stiffness [2].

Unlike the commonly used hot-pressing process, resulting in composites with the shape of plates or shells [3 to 5], the coextrusion technique, developed at the Lehrstuhl für Werkstoffkunde und Mechanische Technologie, Universität Kaiserslautern (FRG), delivers specimens with high aspect ratios [6 and 7]. For the first time extrusion has been used for the manufacture of short-fibre reinforced glasses [8 and 9]. Materials with discontinuous fibres, as opposed to endless-fibre composites, allow nearly total freedom in shaping of parts, and in most cases also their manufacture is much easier and simpler. These advantages compensate the somewhat lower reinforcement effect. The special suitability of the extrusion process for manufacturing short-fibre composites is proved by the fact that during extrusion the fibres get preferably oriented in parallel position with regard to the pressing direction, due to the viscous flow of the glass melt within the extrusion press.

Received July 22, 1991.

[1]) This paper is based on the doctoral thesis by K. Langhans [1], which has been approved by the Department of Material Science and Mechanical Engineering of the University Kaiserslautern (FRG).

[2]) Now with: Andreas Stihl, Waiblingen (FRG).

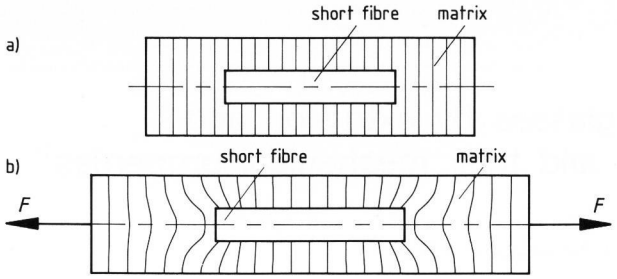

Figures 1a and b. Schematic presentation of a short-fibre composite in the neighbourhood of a single fibre, a) unloaded, b) loaded by tensile stress, $E_f > E_m$. F = force.

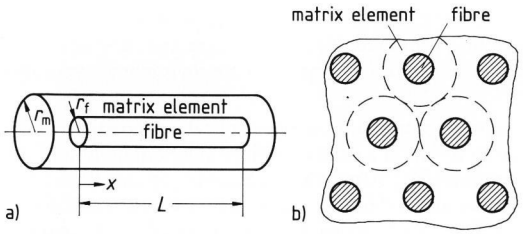

Figures 2a and b. Model for calculating the stress distribution in a short fibre (figure a) and embedding this model in the total composite (figure b).

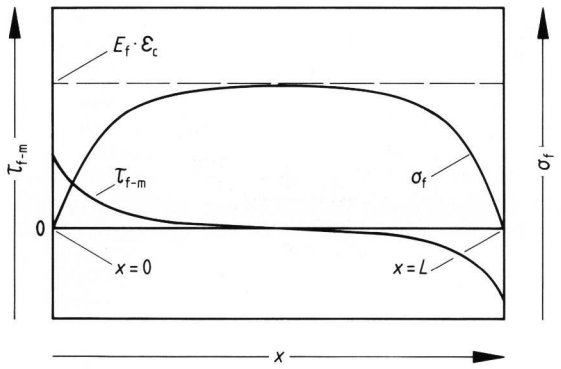

Figure 3. Progression of tensile stress, σ_f, in the fibre and of the shear stress, $\tau_{f\text{-}m}$, at the fibre boundary (according to [11]) as a function of the variable x which corresponds to the fibre length.

2. Theoretical aspects of short-fibre reinforcement

In case of composites with continuous fibres the strains of fibres and matrix can be presumed to be the same over the complete specimen with a high degree of approximation. This assumption results in the basic equation for fibre composites, the so-called linear rule of mixture:

$$E_c = E_f \cdot v_f + E_m \cdot v_m\,, \tag{1}$$

$$\sigma_c = \sigma_f \cdot v_f + \sigma_m \cdot v_m \tag{2}$$

with E = Young's modulus, v = volume fraction, σ = stress, and the indices c = composite, f = fibre, m = matrix.

In short-fibre composites, however, there occur inhomogeneities of deformations, as schematically shown in figures 1a and b for tensile stresses. Especially near the ends of fibres these inhomogeneities, resulting from the different elasticity moduli, can clearly be seen.

For the computation of the distribution of stress in a short fibre, according to Cox [10] and Kelly [11] the model in figures 2a and b is used. This model consists of a single fibre with the length L and the surrounding matrix. The whole composite is under the homogeneous strain, ε_c, parallel to the fibre axis, but the condition of uniform elongation and tension is locally disturbed by the transmission of load onto the fibres.

On condition that this stress transmission only is possible via shear stresses at the cylinder surface of the fibre, but not by normal stresses at the fibre ends, this model results in the following relation for the fibre tensile stress:

$$\sigma_f(x) = E_f \cdot \varepsilon_c \cdot \left[1 - \frac{\cosh(\beta \cdot (L/2 - x))}{\cosh(\beta \cdot L/2)}\right]. \tag{3}$$

From that follows, for the interfacial shear stress $\tau_{f\text{-}m}$:

$$\tau_{f\text{-}m}(x) = \frac{\sigma_f}{2} \cdot \beta \cdot E_f \cdot \varepsilon_c \cdot \frac{\sinh(\beta \cdot (L/2 - x))}{\cosh(\beta \cdot L/2)}. \tag{4}$$

The value β in equations (3 and 4) includes the geometrical data of the model and the elasticity constants of the composite components. In [11 to 13], different expressions for β are indicated, which have all a proportionality $\beta \sim \sqrt{(G_m/E_f)}$ (with G_m = shear modulus of the matrix) in common. The curves of both stresses are schematically shown in figure 3. This schematic representation clearly shows that the reinforcement effect with short fibres is less efficient as compared to continuous fibres, which show the stress $\sigma_f = E_f \cdot \varepsilon_c$ all over their length according to the linear rule of mixture.

For the computation of the Young's modulus the deformation inhomogeneities of the matrix strains are neglected and the average fibre stress $\overline{\sigma_f}$ is inserted into the rule of mixture. With equation (3), this value is:

$$\overline{\sigma_f} = 1/L \int_{x=0}^{L} \sigma_f(x)\,dx = E_f \cdot \varepsilon_c \cdot \left[1 - \frac{\tanh(\beta \cdot L/2)}{(\beta \cdot L/2)}\right]. \tag{5}$$

Thus, for the Young's modulus of the composite follows:

$$E_c = E_f \cdot v_f \cdot \left[1 - \frac{\tanh(\beta \cdot L/2)}{(\beta \cdot L/2)}\right] + E_m \cdot v_m\,. \tag{6}$$

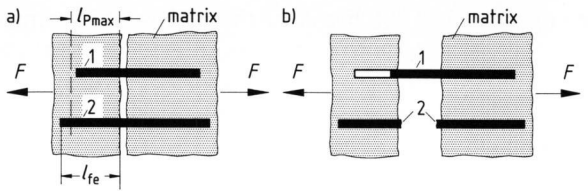

Figures 4a and b. Behaviour of two fibre ends with different lengths at the occurrence of a matrix crack; case 1: length of the fibre end $l_{fe} < l_{Pmax}$: pull out, case 2: length of the fibre end $l_{fe} > l_{Pmax}$: brittle fibre failure; a) matrix crack, b) pull out in case 1 and fibre crack in case 2.

With sufficiently long and slim fibres, the reduction factor in these equations assumes negligibly low values, so that there is only a small difference, as compared to long-fibre composites.

In this reflection it has been silently assumed that the boundary between fibre and matrix is able to transmit the shear stress without a loss of interfacial adhesion. For the fracture behaviour of composites with brittle matrices, however, it is desirable to have a somewhat limited adhesion. Thus, it gets possible to pull the fibres out of the matrix when a crack occurs in it (figures 4a and b, case 1). At this so-called pull out a high amount of friction energy is dissipated, raising the total fracture energy and giving the composite a pseudo-plastic failure behaviour [14 and 15].

When a piece of a fibre with the length, l_P, and the fibre radius, r_f, is pulled out of the surrounding matrix by the external force, F, against a Coulomb friction stress, $\tau = \mu p$, resulting from a radial shrinkage pressure, p, the friction energy

$$W_P = \int_0^{l_P} F(l)\,\mathrm{d}l = \int_0^{l_P} \mu \cdot p \cdot 2\,\pi \cdot r_f \cdot l \cdot \mathrm{d}l = \\ = \mu \cdot p \cdot \pi \cdot r_f \cdot l_P^2 \qquad (7)$$

is dissipated where μ means the coefficient of Coulomb friction. The pull-out length, l_P, however, is limited in upward direction by the ultimate fibre strength, σ_{fu}, and the maximum fibre-matrix shear stress $\tau_{f\text{-}m,\,max}$:

$$l_{Pmax} = \frac{\sigma_{fu} \cdot r_f}{2\,\tau_{f\text{-}m,\,max}} \qquad (8)$$

and with pure friction, respectively:

$$l_{Pmax} = \frac{\sigma_{fu} \cdot r_f}{2\,\mu \cdot p}\,. \qquad (9)$$

If both fibre ends have a distance of more than l_{Pmax} from the crack (figures 4a and b, case 2), the fibre will break brittly in the crack plane and thus almost does not contribute to an increase of fracture energy. That means that a fibre can only be pulled out definitely if its length does not exceed twice the value of l_{Pmax}. The pull-out lengths, l_P, in the crack plane will be distributed between 0 and $L/2$. Therefore, the average pull-out work of one fibre can be calculated by

$$\overline{W}_P = 2/L \int_0^{L/2} \mu \cdot p \cdot \pi \cdot r_f \cdot l_P^2\,\mathrm{d}l_P = \\ = \mu \cdot p \cdot \pi \cdot r_f \cdot L^2/12\,. \qquad (10)$$

For the specific work of friction, related to the cross-sectional area of the composite

$$A_c = \frac{\pi \cdot r_f^2}{v_f}\,,$$

follows

$$w_P = \frac{\overline{W}_P}{A_c} = \frac{v_f}{\pi \cdot r_f^2} \cdot \mu \cdot p \cdot \pi \cdot r_f \cdot \frac{L^2}{12} \qquad (11)$$

for $L < 2\,l_{Pmax}$. Ideally, when the fibre is exactly twice the maximum pull-out length, the result is:

$$w_P = \frac{v_f}{\pi \cdot r_f^2} \cdot \mu \cdot p \cdot \pi \cdot r_f \cdot \frac{l_{Pmax}^2}{3} = \\ = \frac{v_f}{12 \cdot \mu \cdot p} \cdot \sigma_{fu}^2 \cdot r_f \qquad (12)$$

for $L = 2\,l_{Pmax}$. If, however, the fibres used for reinforcement are longer than $2\,l_{Pmax}$, according to Helfet and Harris [16] only the fraction $2\,l_{Pmax}/L$ can be pulled out. Thus, equation (12) changes to:

$$w_P = \frac{2\,l_{Pmax}}{L} \cdot \frac{v_f}{12 \cdot \mu \cdot p} \cdot \sigma_{fu}^2 \cdot r_f = \\ = \frac{1}{L} \cdot \frac{v_f \cdot \sigma^3{}_{fu} \cdot r_f^2}{12 \cdot \mu^2 \cdot p^2} \qquad (13)$$

for $L > 2\,l_{Pmax}$. An analysis of these equations shows two relationships. The first fact is that the pull-out energy and thus the whole fracture energy decreases with an increasing degree of adhesion between fibres and matrix, so that the desired limited degree of adhesion between the components can be explained. Furthermore, it can be seen that surprisingly the specific friction energy decreases with an increasing fibre length, if this value is more than $2\,l_{Pmax}$. In case of long-fibre composites, which nevertheless mostly show a higher work of fracture than short-fibre composites, there appear other energy-dissipating mechanisms which shall, however, not be considered here [7 and 17].

Table 1. Comparison of the most important properties of the composite components [18 to 21]

	AR glass	Nicalon fibre
Young's modulus in N/mm^2	73 000	180 000
strength in N/mm^2	73	2 400
elongation at rupture in %	0.1	1.3
Poisson number	0.22	0.17
density in g/cm^3	2.52	2.55
thermal expansion coefficient in 10^{-6}/K	9.0	3.1

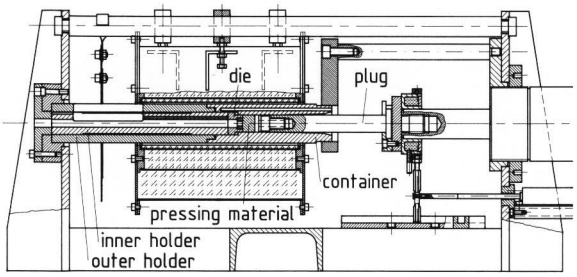

Figure 5. Sectional view of the laboratory extrusion press used in this work.

3. Properties of the components

AR glass, an alkali–lime–silica glass (Schott Glaswerke, Mainz (FRG)), and Nicalon SiC fibres (Nippon Carbon Ltd., Tokyo (Japan)) were chosen as components for the composite. The AR glass is delivered as a powder, 99 % of the particles being smaller than 60 µm and 50 % smaller than 10 µm [18]. The Nicalon short fibres are supplied with an average length of 1 mm, and their diameter is about 15 µm [19]. They are produced by cutting them from endless-fibre bundles. Each of these bundles, also called "rovings", consists of 500 single fibres, and is coated with a polymer size which is a protection for the fibres and a coupling agent in polymer matrices [20].

The comparison shown in table 1 proves that the fibres are a well-suited reinforcing component for AR glass with respect to the mechanical properties. In regard to Young's modulus, strength, and elongation at rupture, they show excellent conditions to improve the mechanical properties of the glass. The considerable difference of the thermal expansion coefficients, which is a feature of a low degree of physical compatibility, is, however, an argument against this combination. During the cooling down from the manufacturing temperature, the fibres get under radial and axial pressure, the matrix, however, under axial and, at the fibre boundaries, under tangential tensile stresses.

This state of stresses results in a good amount of friction between fibres and matrix, but in brittle matrix materials internal tensile stresses are disadvantageous, since they lower the strain of the composite until the break of the matrix. An estimation of the axial tensile stresses shows values which are similar to the strength of bulk glass. Nevertheless, inside the specimens no cracks, caused by this phenomenon, could be found. As also Brückner [22] supposes, one reason for that can be seen in the fact that the strength of the thin glass layers between the fibres can rather be compared with the strength of glass fibres than with the strength of compact glass.

4. Manufacture of the composites

For the success of the extrusion as well as for the quality of the resulting samples, it is indispensable to mix the silicon-carbide short fibres with the AR-glass powder in an extremely homogeneous way. Due to various reasons, however, this is very difficult [23]. One problem is the bulk factor of the fibres and their high tendency to form clews. A second reason for the difficult miscibility features is the very different geometry of the components to be mixed. Thus, it is inevitable that some fibres break during the mixing process. It must, therefore, be the aim of the mixing process to reach homogeneous mixtures in such a way fibres are preserved as much as possible and the formation of clews is avoided or existing clews are destroyed. After many variations of the mixing parameters, the following process proved to be suitable.

First of all, sized fibres are cleaned in an ultrasonic bath with distilled water. Subsequently, the roving pieces are mixed with the glass powder, using a laboratory-type mixing propeller and adding distilled water again. The still existing fibre size protects the fibres at the beginning of the process without avoiding their necessary singularisation until the end. In addition to this, also the forming of clews can be nearly forestalled. Moreover, it is advantageous to dissolve about 2 wt% of hydroxyethylcellulose (HEC) in the distilled water and raise its viscosity considerably in this way. So the flow of the powder-fibre dispersion is much less turbulent, whereby the danger of clew forming and fibre breaking is nearly reduced. Neither the polymer size nor the HEC has a negative effect on the properties of the composites, hence the decomposition temperatures of both materials are much lower than the extrusion temperatures and they are removed during heating up. Moreover, there are some indications that the chemical processes during the decomposition lower the oxidic deterioration of the fibres by consuming the oxygen in the mixture and producing a kind of inert-gas atmosphere. After the mixing process the mixture is being dried and filled into the container of the extruding press.

This machine can be seen in figure 5, in a sectional view. Container, inner and outer holder, die holder,

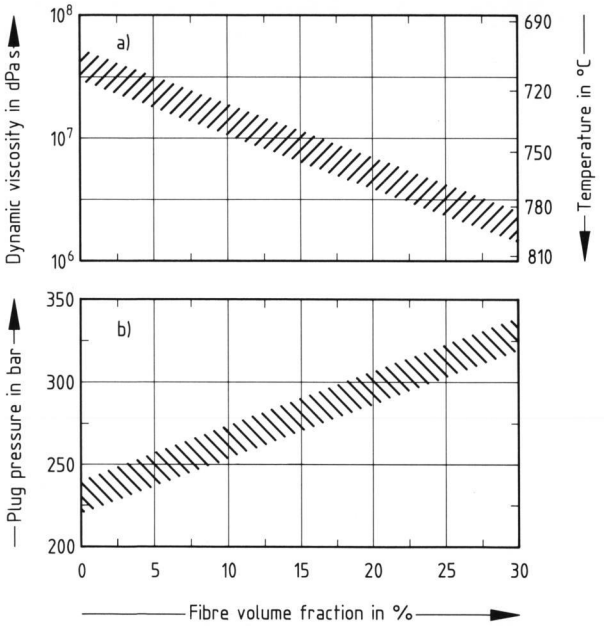

Figures 6a and b. Temperature and viscosity ranges (figure a) and pressures (figure b) suitable for extrusion as a function of fibre-volume fraction.

and plug are made of a high-temperature resistant steel (X 10 Cr Ni 18 10), the plug having a gliding ring made of cast iron at the top. The die is manufactured of electrographite, a material with which the glass melt does not bond. The electric-resistance furnace can produce temperatures up to 900 °C inside the container, and for its regulation there is a thermocouple element installed in the wall of the container, near the deformation zone. The hydraulic plunger, that can partly be seen on the right side, can produce a plug pressure of more than 500 bars.

After filling into the container, the glass powder-fibre mixture is heated up to the pressing temperature and precompressed at a low plug pressure. Thereafter, the required pressure is adjusted and the now compact block is transformed into a rod. Figures 6a and b show the temperature and thus the viscosity ranges and the pressure amounts as a function of the fibre-volume fraction, that have proved to be successful during the experiments. It can clearly be seen that with an increasing fibre fraction the pressing temperatures as well as the pressure have to be raised to get comparable extrusion velocities.

5. Structural examinations of the composite samples

Figure 7 shows a polished cross-section of a glass-composite rod produced as described in section 4. with a fibre-volume fraction of 25 %. The homogeneous distribution of the fibres and the low degree of porosity in the rod can clearly be seen. The examinations of the cross-section with an automatic image-analysing system (TAS plus, Wild-Leitz,

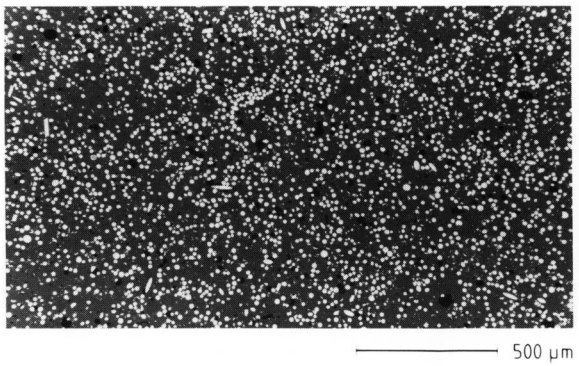

Figure 7. Polished cross-section of an extruded short-fibre reinforced AR-glass rod ($v_f = 25$ %).

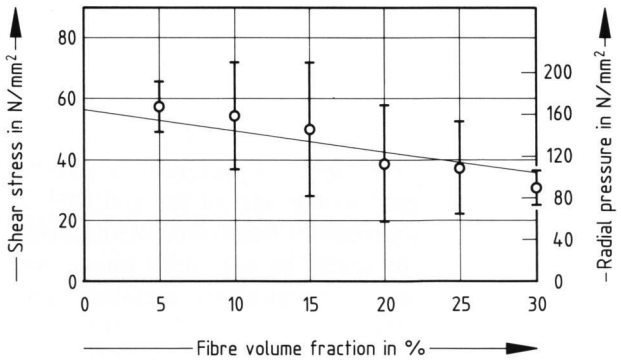

Figure 8. Comparison of the measured shear stresses at the fibre – matrix boundaries (○) with the calculated thermally induced radial shrinkage pressure stresses (—) as a function of fibre-volume fraction.

Wetzlar (FRG)) [24] confirm these impressions also quantitatively. The porosity values, as determined, are about 2 to 7 %, the fibre-volume fraction shows only small straggling over the cross-section.

Another examination at the cross-sections was made with regard to the shear strength at the fibre-matrix boundaries. The method, as used, has been developed by Marshall [25 and 26] and is based on Vickers-microhardness testing. With the aid of this method, that cannot be described here in a detailed way, it is possible to determine the boundary-shear stresses on the basis of the force applied and of the thus caused lowering of the fibre to a level below the cross-section plane. The results of these measurements are demonstrated in figure 8; they show a nearly linear decrease with increasing fibre fraction. A comparison of these values with the results of approximate computations of the thermally caused radial shrinkage pressures, also shown in figure 8, yields an interesting relationship. There is a clear correspondence of the dependences of these two values on the fibre-volume fraction. This allows the conclusion that stress transmission between the AR-glass matrix and the SiC fibres mainly is based on the Coulomb-friction effect and that other bonding mechanisms are at best of subordinate importance. Thus, the maximum boundary-shear stress can be

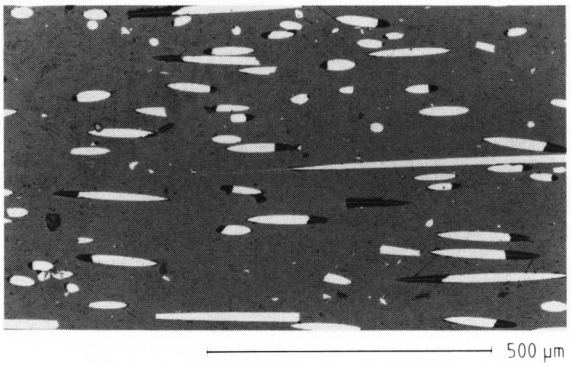

Figure 9. Longitudinal polished section of an extruded short-fibre reinforced glass rod ($v_f = 10$ %).

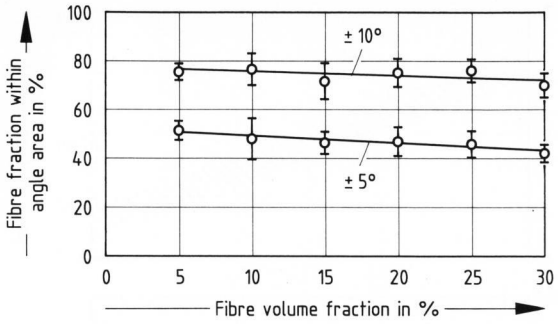

Figure 10. Fractions of analyzed fibres with an angle difference of less than ± 5° and ± 10°, respectively, to the rod axis as a function of fibre-volume fraction.

expressed as $\tau = \mu p$ with a mean coefficient of friction of $\mu = 0.34$ resulting therefrom.

As already mentioned in section 1., the special suitability of extrusion for the manufacture of short-fibre reinforced glasses is to be found in the fact that the fibres adjust themselves preferably in parallel direction with regard to the axis of the rod [27]. A judgement of this alignment behaviour of the fibres was also possible by using the automatic image-analysing system, but at longitudinal metallographic sections of the samples. Although the impression, when inspecting such an image, as shown in figure 9, seems to be unequivocal, it is not unproblematic to judge the alignment objectively.

Especially for this purpose a programme has been developed for the image-analysing system which is able to analyze a longitudinal section independently with regard to fibre orientation. This programme first of all computes an aspect ratio for each fibre section to exclude such sections that are not suitable for an orientation analysis. These can be fibre fragments, cut by the ground surface, but also fibres that are oriented nearly normally to the plane of the section. Subsequently, the end points of all remaining fibre areas, in the direction of the rod axis, are registered, and the angle of the straight line connecting these points with the axis is being calculated. The output of the fibre orientation determined in this way is numerical and – if wanted – graphical. The graphic representation of a good fibre orientation is similar to a narrow Gaussian distribution curve.

For comparing the various angle distributions, the fibre fractions lying inside an angle region of ± 5° and ± 10°, respectively, at this two-dimensional analysis, are being used. Both fractions are slightly decreasing with increasing fibre-volume fraction as figure 10 shows.

6. Determination of mechanical properties of the composites

Besides those structural examinations the specimens were also subjected to investigations with the aim of determining their mechanical properties and their fracture behaviour. Since the tensile test used as a rule for many metallic materials is connected with a couple of problems in case of brittle materials, bending tests were chosen in the present case, as usually. For determining Young's modulus and strength, four-point bending was used, and impact-bending tests offered information about the composites' fracture behaviour.

The four-point bending test was carried out on a computer-controlled universal testing machine according to DIN EN 100 [28]. Compared to three-point bending, where the maximum bending

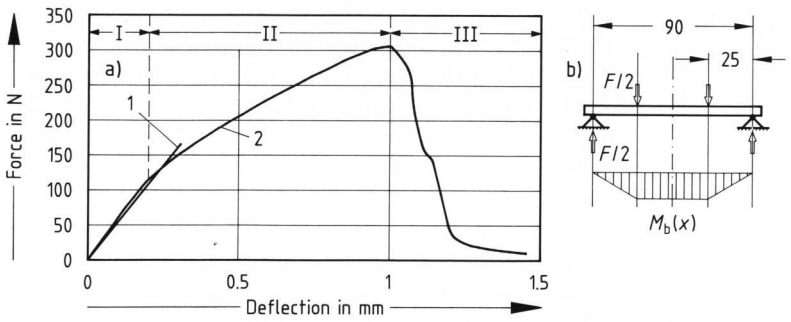

Figures 11a and b. Typical load-deflection diagram drawn after measured values of the four-point bending method and respective equipment; a) load-deflection diagram of non-reinforced (curve 1, $v_f = 0$ %) and short-fibre reinforced (curve 2, $v_f = 30$ %) glass (I = linear-elastic range, II = pseudo-elastic range, III = crack range), b) four-point bending equipment. Shapes of specimens are cylindric with a length of 100 and a diameter of 6 mm. All other dimensions are also given in mm. M_b = bending moment.

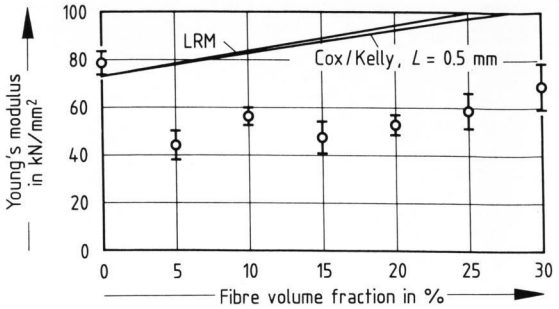

Figure 12. Young's moduli of extruded short-fibre reinforced glass composites as a function of fibre-volume fraction. LRM = Linear Rule of Mixture.

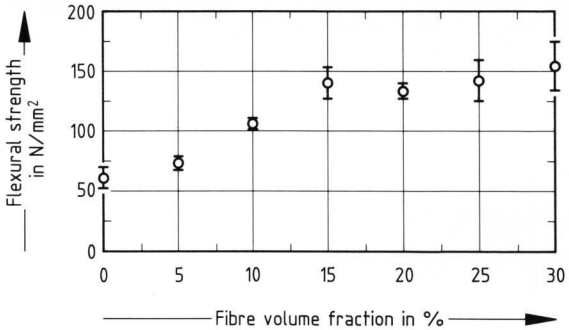

Figure 13. Bending strength of extruded short-fibre reinforced glass composites as a function of fibre-volume fraction.

moment is at one point, this kind of load has the advantage that there is a constant moment without the influence of shearing forces over the complete range between the two load points. Thus, a higher degree of measuring precision can be obtained. Figures 11a and b show a typical load-deflection curve of a composite in comparison to non-reinforced glass (figure a) and the used four-point bending equipment (figure b). The glass specimen was also produced by extrusion of glass powder to ensure comparable conditions. This specimen shows the typical ideal brittle behaviour with a correspondingly low work of fracture that can be determined from the area below the graph. Until the fracture itself, no unelastic deformation of the material can be seen.

In case of fibre-reinforced glass, however, even after exceeding the strain of rupture of the matrix glass and the appearance of the first matrix crack, further load is necessary to destroy the specimen totally. This pseudo-plastic behaviour mainly causes a clearly raised work of fracture.

In principle, such a load-deflection curve can be divided in three areas. At the beginning, at low loads, a linear-elastic behaviour can be seen. That ends with the appearance of the first matrix crack at the tensile-stress side of the specimen. This crack is impeded in its expansion and slowly grows toward the pressure side, during the further loading process. In the already broken region, only the crack-bridging fibres are carrying load. This second phase thus is connected with a continuous decrease of the specimen's stiffness, recognizable by the decreasing of the curve gradient. When the crack at last has parted the whole glass matrix, only those fibres, which have a low degree of bending rigidity, cause the connection of the specimen fragments. That results in a rapid decrease of the bending stiffness in the third phase, but – furthermore – energy is needed to pull the crack-bridging fibres out of the matrix and thus cause the total separation of the specimen.

In the quasi-statical bending test essentially two values are determined that are interesting for judging the composites: the Young's modulus for the behaviour in the Hooke's area and the maximum supportable bending stress. The Young's modulus, which, according to the model described in section 2., should be only negligibly smaller than the corresponding value of long-fibre composites, unfortunately could not fulfil the expectations. The determined values always were much lower than the calculated ones, as can clearly be seen in figure 12. Even the stiffness of non-reinforced glass only sometimes could nearly be reached at high fibre fractions. The reason for that is to be found in the considerable difference of the thermal expansion coefficients. The high internal tensile stresses within the matrix caused thereby can, in connection with surface microcracks, weaken the material even at comparatively small loads and thus decrease the amount of stiffness.

The bending strengths, as related to the original cross-section, however, show much better results (figure 13). These values continuously rise up to 15 vol.% fibres to more than twice the quantity of non-reinforced glass. The stagnation of the ascent recognizable at high fibre fractions mainly can be traced back to the rising problems in mixing and to the increasing amount of fibre damage. Besides that, partially rather clear fluctuations of the fibre properties are quite an important factor. This can be seen from the fact that the highest measured values even with high fibre-volume fractions do not show any stagnation.

The impact-bending test is used to determine the behaviour of materials at shocklike loads which especially in case of brittle matrices can cause critical stresses. Therefore, also the fibre-reinforced glasses were subjected to that test which can yield valuable results in a short time and with few specimen preparations. The value measured in this test is the work of fracture from which the so-called impact resistance a_n is calculated. This is displayed in figure 14 as a function of the fibre-volume fraction. In this case, too, a stagnation can be seen at higher fibre fraction, but not below 20 %. In a way similar to the bending strength, the highest measured quantities show a continuous increase up to 25 %. This difference also has to be traced back to the varying fibre properties.

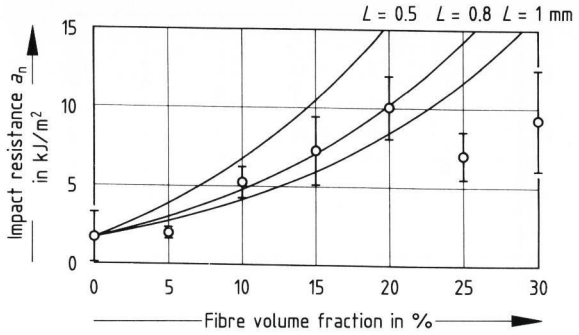

Figure 14. Impact-resistance values of extruded short-fibre reinforced glass composites determined (○) and calculated (—) for different fibre lengths (equation (14)) as a function of fibre-volume fraction.

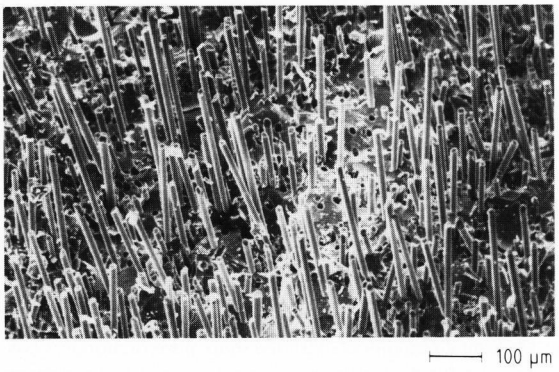

Figure 15. Fracture surface of an impact-bending specimen with pull out of fibres ($v_f = 20\ \%$).

A very interesting relation results by adding the impact resistance of non-reinforced glass, a_{ng}, which is also made by extrusion of glass powder, and the calculated pull-out energy, both multiplied by the corresponding volume fractions. Since the fibre length even after some fibre damage is much higher than $2\,l_{Pmax}$, equation (13) has to be used for this calculation:

$$a_n = \frac{1}{L} \cdot \frac{\sigma_{fu}^3 \cdot r_f^2}{12\,\mu^2 \cdot p^2} \cdot v_f + a_{ng} \cdot v_m \,. \qquad (14)$$

The results of these calculations for different fibre lengths are also displayed in figure 14. The great similarity of the tendencies of the measured and of the calculated values and the nearly exact conformity with the calculation for 0.8 mm long fibres allow the conclusion that indeed the surface energy of the non-reinforced glass and the pull-out energy are mainly responsible for the quantity of work dissipated in impact bending.

Scanning electron microscopic photographs of fracture surfaces of impact-bending specimens (figure 15) show the fibre ends typical for the pull-out process as well as the channels out of which the fibres of the corresponding specimen piece have been pulled. Moreover, these pictures, too, clearly show the parallel orientation of the short fibres within the composite.

7. Summary

The extrusion technique, used for the first time for the manufacture of short-fibre reinforced glasses, has proved to be very suitable for this purpose. Its special advantage lies in the experimentally verified preferred orientation of the fibres in the direction of extrusion. The specimens, as produced, show clear advantages, compared to non-reinforced glass, with regard to strength and fracture toughness. These eventually can even be increased by further optimization of the manufacturing process. Especially, a possible further development of mixing with regard to higher fibre fractions and the possibility of extrusion in vacuum should be mentioned here. Moreover, the investigations should be expanded to other fibre-matrix combinations.

The combination of the properties of fibre-reinforced glasses – here once more low density, limited thermal and extremely high chemical resistance, high hardness and wear resistance, and clearly improved mechanical properties compared to non-reinforced glass should be mentioned – is not reached by any conventional material. For that reason, short-fibre reinforced glasses seem to be suitable for special applications in aeronautics and astronautics, in chemical and medical techniques, in universal engineering and manufacture of apparatus, and in structural glazing, for example in the building trade.

8. References

[1] Langhans, K.: Theoretische und experimentelle Untersuchungen zur Herstellung stranggepreßter kurzfaserverstärkter Gläser sowie zu ihrer Struktur und ihren mechanischen Eigenschaften. Universität Kaiserslautern, Diss. 1991.

[2] Grünthaler, K.-H.; Harkort, D.; Nixdorf, J.: Möglichkeiten zur Verbesserung der Eigenschaften von Glas, Email und Keramik durch Anwendung des Verbundprinzips. Glas-Email-Keramo-Tech. **21** (1970) no. 9, p. 313–324.

[3] Sambell, R. A. J.; Bowen, D. H.; Phillips, D. C.: The technology of carbon-fibre-reinforced glasses and ceramics. In: Carbon fibres. Their place in modern technology. Proc. Int. Conf. London: The Plastics Institute 1974. p. 105–113.

[4] Prewo, K. M.; Brennan, J. J.; Layden, G. K.: Fiber reinforced glasses and glass-ceramics for high performance applications. Am. Ceram. Soc. Bull. **65** (1986) no. 2, p. 305–313, 322.

[5] Pannhorst, W.; Hegeler, H.; Reich, C. et al.: Faserverstärkte Gläser und Glaskeramiken. In: Proc. Verbundwerk, Wiesbaden 1988. p. 9.00–9.13.

[6] Semar, W.: Herstellung SiC-faserverstärkter Glasverbundkörper durch das Strangpreßverfahren und Untersuchung ihrer charakteristischen mechanischen Eigenschaften. Universität Kaiserslautern, Diss. 1986.

[7] Klein, N.: Herstellung stranggepreßter langfaserverstärkter Glasverbundkörper und Untersuchung ihres Werkstoffver-

haltens bei ruhender und schwingender Beanspruchung. Universität Kaiserslautern, Diss. 1990.
[8] Roeder, E.; Klein, N.; Langhans, K.: Manufacture of glass composites reinforced with long and short fibres by extrusion. Glastech. Ber. **61** (1988) no. 5, p. 143–148.
[9] Roeder, E.; Klein, N.; Langhans, K.: Manufacture of fibre-reinforced glass composites by extrusion. Ind. Céram. (1988) no. 3 (825), p. 160–163.
[10] Cox, H. L.: The elasticity and strength of paper and other fibrous materials. Br. J. appl. Phys. **3** (1952) p. 72–79.
[11] Kelly, A.: Werkstoffe hoher Festigkeit. Braunschweig: Vieweg 1973. p. 94 ff.
[12] Dow, N. F.: Study of stresses near a discontinuity in a filament-reinforced composite material. General Electric Company, Missile and Space Division. 1963. Report no. TISR 63SD61.
[13] Rosen, W.: Mechanics of composite strengthening. In: Fiber composite materials. Am. Soc. Metals, 1965. p. 37–75.
[14] Phillips, D. C.: Interfacial bonding and the toughness of carbon fibre reinforced glass and glass-ceramics. J. Mater. Sci. **9** (1974) p. 1847–1854.
[15] Harris, B.; Beaumont, P. W. R.; Moncunill de Ferran, E.: Strength and fracture toughness of carbon fibre polyester composites. J. Mater. Sci. **6** (1971) p. 238–251.
[16] Helfet, J. L.; Harris, B.: Fracture toughness of composites reinforced with discontinuous fibres. J. Mater. Sci. **7** (1972) p. 494–498.
[17] Spallek, M.; Pannhorst, W.: Starke Partner für Hochtemperaturverbundwerkstoffe. Werkst. Konstr. **3** (1989) p. 505–508.
[18] Schott Ruhrglas, Bayreuth: Informationsblatt AR-Glas.
[19] Nippon-Carbon Co., Tokyo (Japan): Inspection sheet of SiC-chopped fiber "NICALON". 1989.
[20] Nippon-Carbon Co., Tokyo (Japan): NICALON – silicon carbide continuous fiber. 1985.
[21] Schott Glaswerke, Mainz: Technische Gläser. Physikalische und chemische Eigenschaften. 1981.
[22] Brückner, R., Berlin: Pers. commun. 1989.
[23] Milewski, J. V.: Efficient use of whiskers in the reinforcement of ceramics. Adv. Ceram. Mater. **1** (1986) p. 36–41.
[24] Klein, N.; Roeder, E.: Untersuchungen SiC-langfaserverstärkter Glasverbunde mit Hilfe der automatischen Bildanalyse. Prakt. Metallogr. **29** (1991) p. 350–358.
[25] Marshall, D. B.: An indentation method for measuring matrix-fiber frictional stresses in ceramic composites. J. Am. Ceram. Soc. **67** (1984) no. 12, p. C-259–C-260.
[26] Marshall, D. B.; Oliver, W. C.: Measurement of interfacial mechanical properties in fiber-reinforced ceramic composites. J. Am. Ceram. Soc. **70** (1987) no. 8, p. 542–548.
[27] Jech, R. W.; Weber, E. P.; Schwope, A. D.: Fiber-reinforced titanium alloys. In: Clough, W. R. (ed.): Reactive metals. New York, London: Interscience Publ. 1958. p. 109–119.
[28] German standard DIN EN 100 (March 1985): Keramische Fliesen und Platten; Bestimmung der Biegefestigkeit. Berlin: DIN 1985.

92R0242